# Switching LPV Control of An F-16 Aircraft via Controller State Reset

Bei Lu
Dept. of Mechanical and Aerospace Engineering, California State University
Long Beach, CA 90840
Fen Wu*
Dept. of Mechanical and Aerospace Engineering, North Carolina State University
Raleigh, NC 27695
SungWan Kim
Dynamic Systems and Control Branch, NASA Langley Research Center
Hampton, VA 23681-2199

**Abstract**

In flight control, the design objective and the aircraft dynamics may be different in low and high angle of attack regions. This paper presents a systematic switching LPV control design method to determine if it is practical to use for flight control designs over a wide angle of attack region. The approach is based on multiple parameter-dependent Lyapunov functions. A family of LPV controllers are designed, and each of them is suitable for a specific parameter subspace. The state of the controller is reset to guarantee the stability requirement of the Lyapunov function when the switching event occurs. Two parameter-dependent switching logics, hysteresis switching and switching with average dwell time, are examined. The proposed switching LPV control scheme is applied to an F-16 aircraft model with different design objectives and aircraft dynamics in low and high angle of attack regions. The nonlinear simulation results using both switching logics are compared.

**Keywords** Switched linear parameter-varying systems; multiple parameter-dependent Lyapunov functions; hysteresis switching; average dwell time; flight control; thrust vector.

*Corresponding author. **E-mail:** fwu@eos.ncsu.edu, **Phone:** (919) 515-5268, **Fax:** (919) 515-7968. This research is sponsored in part by the NASA Langley Research Center under the grant NAG-1-01119.

# 1 Introduction

In flight control, different performance goals are often desirable for different angle of attack regions. For example, in a low angle of attack scenario, pilots desire fast and accurate responses for maneuvering and attitude tracking. While in a high angle of attack region, the flight control emphasis lies in the maintainability of aircraft stability with acceptable flying qualities. A modern fighter aircraft usually works in a wide angle of attack region, even near stall or poststall regime. In such a case, it is difficult to design a single robust controller over the entire flight envelope. Typically, the controller is designed by compromising the performance in some angle of attack region.

Another issue encountered in flight control is that the actuator dynamics may be different in low and high angle of attack regions. It is known that the redundant control effectors, such as thrust vectoring nozzles, are usually incorporated in the high angle of attack region to provide additional control power. The usual way to generate the thrust vectoring command is a two-step procedure. A controller is designed first based on the generalized control, and the real control input is then generated using a control selector [1, 2, 3, 4]. It has not been clearly addressed how to develop the control law with guaranteed stability and performance by considering the aerodynamic force and thrust force in a unified frame.

To solve those problems, this paper considers a switching linear parameter-varying (LPV) control technique to design a family of controllers, each suitable in different angle of attack region, and switch among them according to the evolution of angle of attack. The whole framework is based on LPV systems because of their relevance to nonlinear systems. The proposed switching LPV control technique is the generalization of results in switched LTI systems. Obviously, stability is an important and challenging problem in switched systems, and it has received considerable attention in the recent literature (see Refs. [5, 6, 7]). For a family of stable LTI systems, the existence of a common Lyapunov function provides sufficient conditions for stability of switched systems under arbitrary switching sequences [8, 6]. However, this kind of stability guarantee is deemed to be too conservative when a particular switching logic is concerned. For restricted class of switching signals, multiple Lyapunov functions have been shown to be very useful tools for stability analysis purpose. Specifically, non-traditional stability conditions have been developed using either piecewise continuous Lyapunov functions [9, 10, 11, 12], or discontinuous Lyapunov functions [13, 14]. In the former case, the values of Lyapunov functions corresponding to the active

subsystems form a decreasing sequence. This constraint is relaxed in the latter one by requiring each Lyapunov function $V_p$ to decrease when the $p$th subsystem is active with possible jump at switching time. The results of switched LTI systems have been generalized to the analysis and control of switched LPV systems [15], which is further extended in Ref. [16] by incorporating average dwell time switching logic [17]. The stability of switched LPV systems was analyzed by multiple parameter-dependent Lyapunov functions, which are allowed to be discontinuous at the switching surfaces.

Recently, the authors have developed switching LPV control techniques under hysteresis and average dwell time switching logics [18]. The multiple parameter-dependent Lyapunov functions [16] are used for analyzing the stability of switched LPV systems. We also considered the optimized performance, which is another important issue and has not been addressed adequately in the most of current work. However, the control synthesis conditions for both switching logics are formulated as non-convex matrix optimization problems, which are difficult to solve. In this research, we will bypass the non-convex condition by resetting the state of the controller when the switching event occurs. If the plant state is measurable, we can assign the controller state equal to the plant state at switching instances to guarantee the stability requirement of the Lyapunov functions. It is noted that the controller state reset is not always a feasible option due to lack of the information of the plant state. In this case, the state of the plant may be estimated by adding an observer. To simplify the theoretical derivation, we assume that the state of the plant is measurable in this research. The effect of an observer and the constraints for the observer design in order to guarantee the exponential stability will be studied in our future research.

The notation is standard. $\mathbf{R}$ stands for the set of real numbers and $\mathbf{R}_+$ for the non-negative real numbers. $\mathbf{R}^{m\times n}$ is the set of real $m \times n$ matrices. The transpose of a real matrix $M$ is denoted by $M^T$. $\mathrm{Ker}(M)$ is used to denote the orthogonal complement of $M$. We use $\mathbf{S}^{n\times n}$ to denote the real symmetric $n \times n$ matrices and $\mathbf{S}_+^{n\times n}$ to denote positive definite matrices. If $M \in \mathbf{S}^{n\times n}$, then $M > 0$ ($M \geq 0$) indicates that $M$ is positive definite (positive semidefinite) and $M < 0$ ($M \leq 0$) denotes a negative definite (negative semidefinite) matrix. For $x \in \mathbf{R}^n$, its norm is defined as $\|x\| := (x^T x)^{\frac{1}{2}}$. The space of square integrable functions is denoted by $\mathcal{L}_2$, that is, for any $u \in \mathcal{L}_2$, $\|u\|_2 := \left[\int_0^\infty u^T(t)u(t)dt\right]^{\frac{1}{2}}$ is finite.

The paper is organized as follows: the problem addressed in this paper is first briefly formulated in Section 2. In Subsection 2.1, we provide the synthesis condition for hysteresis switching LPV

control via controller state reset, and the result for switching with average dwell time is provided in Subsection 2.2. The proposed technique is applied to an F-16 longitudinal flight control system with thrust vector augmentation in Section 3. The nonlinear simulations of the closed-loop system under these two switching logics are presented and also compared. Finally, the paper concludes in Section 4.

## 2 Switching LPV Control via Controller State Reset

Consider a generalized open-loop LPV system as functions of the scheduling parameter $\rho$. It is assumed that $\rho$ is in a compact set $\mathcal{P} \subset \mathbf{R}^s$ with its parameter variation rate bounded by $\underline{\nu}_k \leq \dot{\rho}_k \leq \overline{\nu}_k,\ k = 1, 2, \cdots, s$. The time-varying parameter value is assumed measurable in real-time. For notational purposes, we denote $\mathcal{V} = \{\nu :\ \underline{\nu}_k \leq \nu_k \leq \bar{\nu}_k,\ \ k = 1, 2, \ldots, s\}$, where $\mathcal{V}$ is a given convex polytope in $\mathbf{R}^s$ that contains the origin. Suppose that the parameter set $\mathcal{P}$ is partitioned into a finite number of closed subsets $\{\mathcal{P}_i\}_{i \in Z_N}$ by means of a family of switching surfaces $\mathcal{S}_{ij}$ $(i, j \in Z_N)$, where the index set $Z_N = \{1, 2, \ldots, N\}$. In each parameter subset, the dynamic behavior of the system is governed by the equation

$$\begin{bmatrix} \dot{x}(t) \\ e(t) \\ y(t) \end{bmatrix} = \begin{bmatrix} A_i(\rho) & B_{1,i}(\rho) & B_{2,i}(\rho) \\ C_{1,i}(\rho) & D_{11,i}(\rho) & D_{12,i}(\rho) \\ C_{2,i}(\rho) & D_{21,i}(\rho) & D_{22,i}(\rho) \end{bmatrix} \begin{bmatrix} x(t) \\ d(t) \\ u(t) \end{bmatrix}, \qquad \forall\ \rho \in \mathcal{P}_i, \tag{1}$$

where the plant state $x \in \mathbf{R}^n$. $e \in \mathbf{R}^{n_e}$ is the controlled output, and $d \in \mathbf{R}^{n_d}$ is the disturbance input. $y \in \mathbf{R}^{n_y}$ is the measurement for control, and $u \in \mathbf{R}^{n_u}$ is the control input. All of the state-space data are continuous functions of the parameter $\rho$. Note that each LPV model should have the same number of state, and the reason will be clarified in the sequel. It is also assumed that

**(A1)** $(A_i(\rho), B_{2,i}(\rho), C_{2,i}(\rho))$ triple is parameter-dependent stabilizable and detectable for all $\rho$.

**(A2)** The matrix functions $[B_{2,i}^T(\rho) \quad D_{12,i}^T(\rho)]$ and $[C_{2,i}(\rho) \quad D_{21,i}(\rho)]$ have full row ranks for all $\rho \in \mathcal{P}_i$.

**(A3)** $D_{11,i}(\rho) = 0$ and $D_{22,i}(\rho) = 0$.

Note that the assumption (**A3**) can be relaxed by loop transformation [19], but the controller formula will become more complicated.

Given the open-loop LPV system (1), it is sometimes hard to find single LPV controller working for the entire parameter region based on a single Lyapunov function (quadratic or parameter-dependent) [20, 21]. Switching LPV control technique permits use of most suitable controllers in different parameter subsets, and switch among them according to the evolution of the parameters. It will be beneficial to improve controlled performance and enhance design flexibility. In the previous research of switching LPV control [18], the state of the controller was preserved before and after switching, and this resulted in non-convex matrix optimization problems. In this paper, the controller state is reset at switching instances. As a result, this modification leads to a linear matrix inequality (LMI) optimization problem, which can be solved efficiently. The switched LPV controllers with state reset are in the form of

$$\begin{cases} \begin{bmatrix} \dot{x}_k(t) \\ u(t) \end{bmatrix} = \begin{bmatrix} A_{k,i}(\rho, \dot{\rho}) & B_{k,i}(\rho) \\ C_{k,i}(\rho) & D_{k,i}(\rho) \end{bmatrix} \begin{bmatrix} x_k(t) \\ y(t) \end{bmatrix}, & \forall\ \rho \in \mathcal{P}_i \\ x_k(t^+) = x(t), & \forall\ \rho \in \mathcal{S}_{ij}, \end{cases} \tag{2}$$

where the dimension of controller state is $x_k \in \mathbf{R}^{n_k}$, and $n_k = n$. Each controller is activated in a specific parameter subset $\mathcal{P}_i$, and the state of the controller evolves continuously within the subset $\mathcal{P}_i$. When the parameter trajectory hits the switching surface $\mathcal{S}_{ij}$, the controller state is reset to the current value of the plant state.

Then the closed-loop LPV system can be described by

$$\begin{cases} \begin{bmatrix} \dot{x}_{cl}(t) \\ e(t) \end{bmatrix} = \begin{bmatrix} A_{cl,\sigma}(\rho, \dot{\rho}) & B_{cl,\sigma}(\rho) \\ C_{cl,\sigma}(\rho) & D_{cl,\sigma}(\rho) \end{bmatrix} \begin{bmatrix} x_{cl}(t) \\ d(t) \end{bmatrix}, & \forall\ \rho \in \mathcal{P}_i \\ x_{cl}(t^+) = [x(t); \quad x(t)], & \forall\ \rho \in \mathcal{S}_{ij}, \end{cases} \tag{3}$$

where $x_{cl} \in \mathbf{R}^{n+n_k}$ with $x_{cl}^T = [x^T \quad x_k^T]$, and $\sigma$ is a switching signal, which is defined as a piecewise constant function. It is assumed that $\sigma$ is continuous from the right everywhere. The value of switching signal $\sigma$ represents the active parameter subset and thus determines the dynamic behavior of the plant and the controller. It is desirable that each controller stabilizes the open-loop system with best achievable performance in a specific parameter region, and meanwhile maintains the stability of the closed-loop system when switching the controller.

A discontinuous Lyapunov function consisting of multiple parameter-dependent Lyapunov functions is used for stability analysis and control design of switched LPV systems. If there exist a family of positive definite matrix functions $\{X_i(\rho)\}_{i \in Z_N}$, and each of them is smooth over the corresponding

parameter subset $\mathcal{P}_i$. The multiple parameter-dependent Lyapunov functions can then be defined as

$$V_\sigma(x,\rho) = x^T X_\sigma(\rho) x. \tag{4}$$

Generally speaking, for a switched LPV system to be stable, the value of the discontinuous Lyapunov function $V_\sigma$ is not necessarily decreasing over the entire parameter trajectory. In fact, it is often enough to require that the value of $V_\sigma$ decreases in the active parameter region $\mathcal{P}_i$ provided proper switching logic is adopted. This will lead to relaxed stability condition and provides enhanced design flexibility. In this section, we consider the synthesis conditions of switching LPV control with two different switching logics by resetting the controller state.

## 2.1 Hysteresis Switching

When hysteresis switching logic is employed, it is assumed that any two adjacent parameter subsets are overlapped, as shown in Figure 1(a). Thus there are two switching surfaces between two adjacent parameter subsets. We use $\mathcal{S}_{ij}$ to denote the switching surface specifying the one-directional move from subset $\mathcal{P}_i$ to $\mathcal{P}_j$.

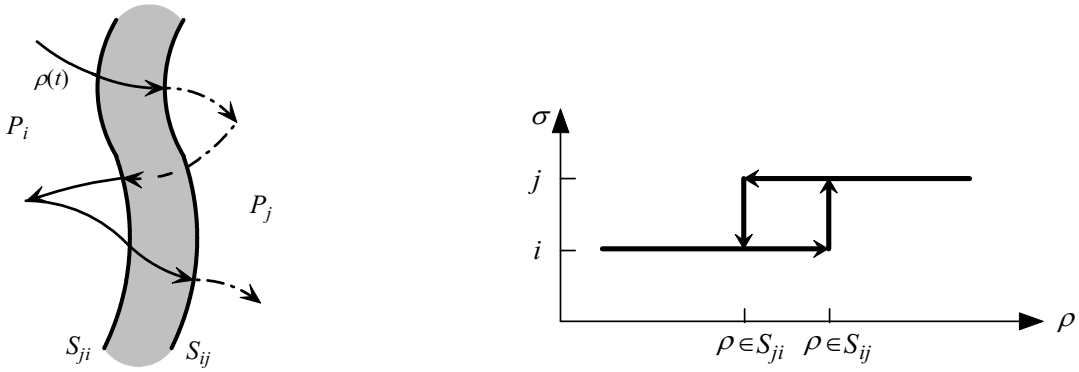


(a) Hysteresis switching region

(b) Hysteresis switching signal

Figure 1: Hysteresis switching region and switching signal $\sigma$.

The switching events occurs when the parameter trajectory hits one of the switching surfaces $\mathcal{S}_{ij}$ or $\mathcal{S}_{ji}$. The evolution of the switching signal $\sigma$ is described as follows. Let $\sigma(0) = i$ if $\rho(0) \in \mathcal{P}_i$. For each $t > 0$, if $\sigma(t^-) = i$ and $\rho(t) \in \mathcal{P}_i$, keep $\sigma(t) = i$. On the other hand, if $\sigma(t^-) = i$ but $\rho(t) \notin \mathcal{P}_i$, i.e., hitting the switching surface $\mathcal{S}_{ij}$, let $\sigma(t) = j$. Similarly, if $\sigma(t^-) = j$ but $\rho(t) \notin \mathcal{P}_j$, i.e., hitting the switching surface $\mathcal{S}_{ji}$, let $\sigma(t) = i$. Obviously, the switching event is parameter-dependent,

as shown in Figure 1(b). For LPV systems, it is conceivable that parameter-dependent switching is more practical than state-dependent or time-dependent switching. Since $\sigma$ changes its value only after the continuous trajectory has passed through the intersection of adjacent subsets $\mathcal{P}_i$ and $\mathcal{P}_j$, chattering is avoided. Also due to bounded parameter variation rates, only finite number of switches will happen in any finite time interval.

For the closed-loop system (3) under the hysteresis switching logic, if on the switching surface $\mathcal{S}_{ij}$, we have $V_i(x_{cl},\rho) \geq V_j([x;x],\rho)$, i.e. the Lyapunov function of the closed-loop system (3) non-increases when switching from $\mathcal{P}_i$ to $\mathcal{P}_j$. Then the $j$th controller can be activated safely. The synthesis condition of switched LPV control with hysteresis switching is given in the following theorem.

**Theorem 1** *Given an open-loop LPV system (1), the parameter set $\mathcal{P}$ and its overlapped partition $\{\mathcal{P}_i\}_{i\in Z_N}$, if there exist positive definite matrix functions $R_i, S_i : \mathbf{R}^s \to \mathbf{S}_+^{n\times n}, i \in Z_N$, such that for any $\rho \in \mathcal{P}_i$,*

$$\mathcal{N}_{R,i}^T(\rho)\begin{bmatrix} R_i(\rho)A_i^T(\rho)+A_i(\rho)R_i(\rho)-\sum_{k=1}^{s}\{\underline{\nu}_k,\overline{\nu}_k\}\frac{\partial R_i}{\partial \rho_k} & R_i(\rho)C_{1,i}^T(\rho) & B_{1,i}(\rho) \\ C_{1,i}(\rho)R_i(\rho) & -\gamma_i I_{n_e} & 0 \\ B_{1,i}^T(\rho) & 0 & -\gamma_i I_{n_d}\end{bmatrix}\mathcal{N}_{R,i}(\rho) < 0 \quad (5)$$

$$\mathcal{N}_{S,i}^T(\rho)\begin{bmatrix} A_i^T(\rho)S_i(\rho)+S_i(\rho)A_i(\rho)+\sum_{k=1}^{s}\{\underline{\nu}_k,\overline{\nu}_k\}\frac{\partial S_i}{\partial \rho_k} & S_i(\rho)B_{1,i}(\rho) & C_{1,i}^T(\rho) \\ B_{1,i}^T(\rho)S_i(\rho) & -\gamma_i I_{n_d} & 0 \\ C_{1,i}(\rho) & 0 & -\gamma_i I_{n_e}\end{bmatrix}\mathcal{N}_{S,i}(\rho) < 0 \quad (6)$$

$$\begin{bmatrix} R_i(\rho) & I_n \\ I_n & S_i(\rho)\end{bmatrix} \geq 0, \quad (7)$$

*where* $\mathcal{N}_{R,i}(\rho) = \mathrm{Ker}\begin{bmatrix} B_{2,i}^T(\rho) & D_{12,i}^T(\rho) & 0\end{bmatrix}$ *and* $\mathcal{N}_{S,i}(\rho) = \mathrm{Ker}\begin{bmatrix} C_{2,i}(\rho) & D_{21,i}(\rho) & 0\end{bmatrix}$, *and for any* $\rho \in \mathcal{S}_{ij}$,

$$R_i(\rho) \leq R_j(\rho), \quad (8)$$

*then the closed-loop LPV system (3) is exponentially stabilized by switched LPV controllers with state reset in the entire parameter set $\mathcal{P}$, and its performance is maintained as $\|e\|_2 < \gamma\|d\|_2$ with* $\gamma = \max\{\gamma_i\}_{i\in Z_N}$.

*Proof:* The proof is similar to that in Ref. [18]. Therefore, we only show that the Lyapunov

function on the switching surface $\mathcal{S}_{ij}$ satisfies $V_i(x_{cl},\rho) \geq V_j([x;x],\rho)$ given the boundary condition (8). Following the idea in Ref. [18], we partition the Lyapunov function matrices of the closed-loop system (3) according to the dimensions of the plant and controller states as

$$X_i(\rho) = \begin{bmatrix} S_i(\rho) & N_i(\rho) \\ N_i^T(\rho) & ? \end{bmatrix}, \qquad X_i^{-1}(\rho) = \begin{bmatrix} R_i(\rho) & M_i(\rho) \\ M_i^T(\rho) & ? \end{bmatrix},$$

where $M_i(\rho)N_i^T(\rho) = I - R_i(\rho)S_i(\rho)$, and "?" means the elements we don't care. By choosing $M_i(\rho) = R_i(\rho)$ and $N_i(\rho) = R_i^{-1}(\rho) - S_i(\rho)$, the Lyapunov function $X_i(\rho)$ can be written as

$$X_i(\rho) = \begin{bmatrix} S_i(\rho) & R_i^{-1}(\rho) - S_i(\rho) \\ R_i^{-1}(\rho) - S_i(\rho) & S_i(\rho) - R_i^{-1}(\rho) \end{bmatrix},$$

which can be further decomposed to

$$X_i(\rho) = \begin{bmatrix} I & -I \\ 0 & I \end{bmatrix} \begin{bmatrix} R_i^{-1}(\rho) & 0 \\ 0 & S_i(\rho) - R_i^{-1}(\rho) \end{bmatrix} \begin{bmatrix} I & 0 \\ -I & I \end{bmatrix}.$$

Therefore,

$$V_\sigma(x_{cl},\rho) = \begin{bmatrix} x^T & (x_k - x)^T \end{bmatrix} \begin{bmatrix} R_\sigma^{-1}(\rho) & 0 \\ 0 & S_\sigma(\rho) - R_\sigma^{-1}(\rho) \end{bmatrix} \begin{bmatrix} x \\ (x_k - x) \end{bmatrix}. \tag{9}$$

Assume that the parameter trajectory hits the switching surface $\mathcal{S}_{ij}$. Then the Lyapunov function before switching is

$$V_i(x_{cl},\rho) = x^T R_i^{-1}(\rho)x + (x_k - x)^T \left(S_i(\rho) - R_i^{-1}(\rho)\right)(x_k - x).$$

Combining with the coupling condition (7) gives

$$V_i(x_{cl},\rho) \geq x^T R_i^{-1}(\rho)x.$$

If the states of the controller are reset when switching, i.e., $x_k = x$, then the Lyapunov function after switching is

$$V_j([x;x],\rho) = x^T R_j^{-1}(\rho)x.$$

Therefore, $V_i(x_{cl},\rho) \geq V_j([x;x],\rho)$ is satisfied at the switching surface $\mathcal{S}_{ij}$ if $R_i^{-1}(\rho) \geq R_j^{-1}(\rho)$, which is equivalent to the boundary condition (8). *Q.E.D.*

Note that the hysteresis-based switching LPV control via controller state reset is formulated as a convex optimization problem, and can be solved using efficient LMI numerical algorithms [22]. It should be pointed out that the functional dependency of matrices $R_i$ and $S_i$ to parameters $\rho_k, k = 1, \ldots, s$ has to be chosen before solving the problem. The notation $\sum_{k=1}^{s} \{\underline{\nu}_k, \bar{\nu}_k\} \frac{\partial}{\partial \rho_k}$ in (5)-(6) represents the combination of derivative terms in the form of $\nu_k \frac{\partial}{\partial \rho_k}$ when $\nu_k$ is taken as either $\underline{\nu}_k$ or $\bar{\nu}_k$. Therefore each inequality means $2^s$ different LMIs which must be checked.

After solving matrix functions $R_i(\rho)$ and $S_i(\rho)$, the gains of switched LPV controllers can be constructed using the following formula [23]

$$\begin{aligned} A_{k,i}(\rho, \dot{\rho}) = -N_i^{-1}(\rho) \Big\{ & A_i^T(\rho) - S_i(\rho)\frac{dR_i}{dt} - N_i(\rho)\frac{dM_i^T}{dt} + S_i(\rho)\left[A_i(\rho)\right. \\ & \left. + B_{2,i}(\rho)F_i(\rho) + L_i(\rho)C_{2,i}(\rho)\right] R_i(\rho) + \frac{1}{\gamma_i} S_i(\rho)\left[B_{1,i}(\rho) + L_i(\rho)D_{21,i}(\rho)\right] B_{1,i}^T(\rho) \\ & + \frac{1}{\gamma_i} C_{1,i}^T(\rho)\left[C_{1,i}(\rho) + D_{12,i}(\rho)F_i(\rho)\right] R_i(\rho) \Big\} M_i^{-T}(\rho) \end{aligned} \tag{10}$$

$$B_{k,i}(\rho) = N_i^{-1}(\rho) S_i(\rho) L_i(\rho) \tag{11}$$

$$C_{k,i}(\rho) = F_i(\rho) R_i(\rho) M_i^{-T}(\rho) \tag{12}$$

$$D_{k,i}(\rho) = 0, \tag{13}$$

where the matrix functions $F_i(\rho)$ and $L_i(\rho)$ defined as

$$\begin{aligned} F_i(\rho) &= -\left(D_{12,i}^T(\rho) D_{12,i}(\rho)\right)^{-1} \left[\gamma_i B_{2,i}^T(\rho) R_i^{-1}(\rho) + D_{12,i}^T(\rho) C_{1,i}(\rho)\right] \\ L_i(\rho) &= -\left[\gamma_i S_i^{-1}(\rho) C_{2,i}^T(\rho) + B_{1,i}(\rho) D_{21,i}^T(\rho)\right] \left(D_{21,i}(\rho) D_{21,i}^T(\rho)\right)^{-1}. \end{aligned}$$

To comply with the proposed controller state reset scheme, we need to choose particular realizations of LPV controllers with $M_i(\rho) = R_i(\rho)$ and $N_i(\rho) = R_i^{-1}(\rho) - S_i(\rho)$.

**Remark 1** *For general specification of $M_i(\rho)$ and $N_i(\rho)$, the synthesis conditions (5)-(8) still hold. However, the controller state on the switching surface $\mathcal{S}_{ij}$ is not simply reset to the plant state. From the structures of the Lyapunov function matrix and its inverse, one can get*

$$X_i(\rho) = \begin{bmatrix} S_i(\rho) & N_i(\rho) \\ N_i^T(\rho) & -N_i^T(\rho) R_i(\rho) M_i^{-T}(\rho) \end{bmatrix}, \qquad \forall\ i \in Z_N.$$

*Combined with the constraint $M_i(\rho) N_i^T(\rho) = I - R_i(\rho) S_i(\rho)$, $X_i(\rho)$ can be decomposed and further simplified to*

$$X_i(\rho) = \begin{bmatrix} I & -R_i^{-1}(\rho) M_i(\rho) \\ 0 & I \end{bmatrix} \begin{bmatrix} R_i^{-1}(\rho) & 0 \\ 0 & -N_i^T(\rho) R_i(\rho) M_i^{-1}(\rho) \end{bmatrix} \begin{bmatrix} I & 0 \\ -M_i^{-T}(\rho) R_i^{-1}(\rho) & I \end{bmatrix}.$$

*Therefore, on the switching surface $\mathcal{S}_{ij}$, the controller state needs to be reset to*

$$x_k(t^+) = M_j^T(\rho)R_j^{-1}(\rho)x(t).$$

## 2.2 Switching with Average Dwell Time

If the overlapped region between two adjacent parameter subsets shrinks, it eventually becomes a single switching surface, as shown in Figure 2(a). Different from hysteresis switching, here $\mathcal{S}_{ij}$ and $\mathcal{S}_{ji}$ represent the same switching surface between subsets $\mathcal{P}_i$ and $\mathcal{P}_j$ regardless which direction the parameter trajectory moves from. As shown in Figure 2(b), the switching signal changes its value right after the parameter hits the switching surface $\mathcal{S}_{ij}$ no matter which direction the parameter evolves from. This usually requires the continuity of Lyapunov function across the switching surfaces. To relax the continuity requirement, we will consider the switching logic with average dwell time [17, 16], and only limited number of switchings is allowed between a finite time interval.

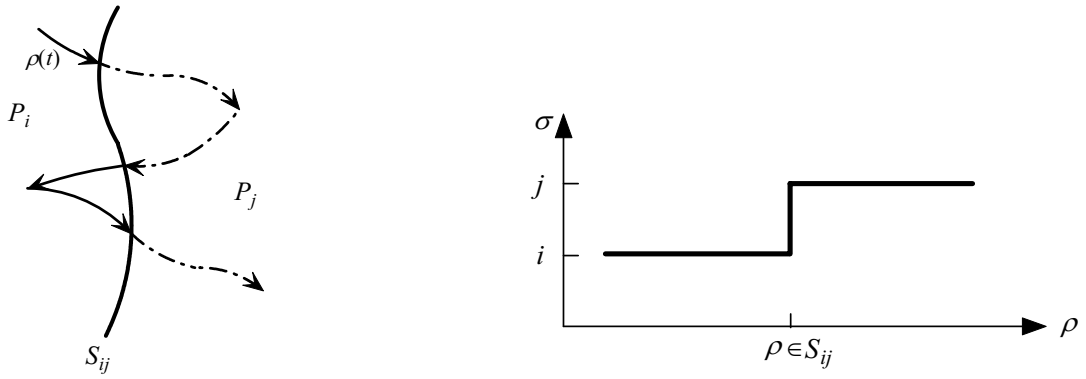


(a) Switching region with dwell time

(b) Switching signal with dwell time

Figure 2: Switching region and switching signal $\sigma$ with dwell time.

Denote $N_\sigma(T,t)$ as the number of switchings among subsets $\mathcal{P}_i$ on an interval $(t,T)$. The switching signal $\sigma$ has average dwell time $\tau_a$ if there exist two positive numbers $N_0$ and $\tau_a$ such that

$$N_\sigma(T,t) \leq N_0 + \frac{T-t}{\tau_a}, \qquad \forall\ 0 \leq t \leq T,$$

where $N_0$ is called the chatter bound. This idea relaxes the concept of dwell time, allowing the possibility of switching fast when necessary and then compensating for it by switching sufficiently slow later on.

Basically, all we need is the fact that there exists a positive constant $\mu$ such that $V_j(\rho) \le \mu V_i(\rho)$ when switching from $\mathcal{P}_i$ to $\mathcal{P}_j$ [7]. Due to the interchangeability of $i$ and $j$, the Lyapunov function on the switching surface must satisfy

$$\frac{1}{\mu} V_j(\rho) \le V_i(\rho) \le \mu V_j(\rho) \qquad \forall\ \rho \in \mathcal{S}_{ij}, \tag{14}$$

where $\mu > 1$. It allows the change of Lyapunov function by $\mu$ times of its value before switching. As a consequence, the average switching frequency over a finite time interval is limited to $\frac{1}{\tau_a}$ to compensate for possible increase of Lyapunov functions.

Different from hysteresis switching, the synthesis condition of switching LPV control with average dwell time cannot be convexified under some conservative assumptions if the control state is preserved when switching [18]. The next theorem shows that the non-convex synthesis condition can be bypassed by resetting the control state. It is an important step for actual implementation, and we will give the detailed proof.

**Theorem 2** *Given scalars $\lambda_0 > 0$, $\mu > 1$, an open-loop LPV system (1), the parameter set $\mathcal{P}$ and its partition $\{\mathcal{P}_i\}_{i \in Z_N}$, if there exist positive definite matrix functions $R_i, S_i : \mathbf{R}^s \to \mathbf{S}_+^{n \times n}, i \in Z_N$, such that for any $\rho \in \mathcal{P}_i$*

$$\mathcal{N}_{R,i}^T(\rho) \begin{bmatrix} \left\{ \begin{array}{c} R_i(\rho) A_i^T(\rho) + A_i(\rho) R_i(\rho) \\ -\sum_{k=1}^{s} \{\underline{\nu}_k, \overline{\nu}_k\} \dfrac{\partial R_i}{\partial \rho_k} + \lambda_0 R_i(\rho) \end{array} \right\} & R_i(\rho) C_{1,i}^T(\rho) & B_{1,i}(\rho) \\ C_{1,i}(\rho) R_i(\rho) & -\gamma_i I_{n_e} & 0 \\ B_{1,i}^T(\rho) & 0 & -\gamma_i I_{n_d} \end{bmatrix} \mathcal{N}_{R,i}(\rho) < 0 \tag{15}$$

$$\mathcal{N}_{S,i}^T(\rho) \begin{bmatrix} \left\{ \begin{array}{c} A_i^T(\rho) S_i(\rho) + S_i(\rho) A_i(\rho) \\ +\sum_{k=1}^{s} \{\underline{\nu}_k, \overline{\nu}_k\} \dfrac{\partial S_i}{\partial \rho_k} + \lambda_0 S_i(\rho) \end{array} \right\} & S_i(\rho) B_{1,i}(\rho) & C_{1,i}^T(\rho) \\ B_{1,i}^T(\rho) S_i(\rho) & -\gamma_i I_{n_d} & 0 \\ C_{1,i}(\rho) & 0 & -\gamma_i I_{n_e} \end{bmatrix} \mathcal{N}_{S,i}(\rho) < 0 \tag{16}$$

$$\begin{bmatrix} R_i(\rho) & I_n \\ I_n & S_i(\rho) \end{bmatrix} \ge 0, \tag{17}$$

*where $\mathcal{N}_{R,i}(\rho) = \mathrm{Ker} \begin{bmatrix} B_{2,i}^T(\rho) & D_{12,i}^T(\rho) & 0 \end{bmatrix}$ and $\mathcal{N}_{S,i}(\rho) = \mathrm{Ker} \begin{bmatrix} C_{2,i}(\rho) & D_{21,i}(\rho) & 0 \end{bmatrix}$, and for any $\rho \in \mathcal{S}_{ij}$*

$$\frac{1}{\mu} R_j(\rho) \le R_i(\rho) \le \mu R_j(\rho), \tag{18}$$

*then the closed-loop LPV system (3) is exponentially stabilized by switched LPV controllers with state reset in the entire parameter set $\mathcal{P}$ for every switching signal $\sigma$ with average dwell time*

$$\tau_a > \frac{\ln \mu}{\lambda_0}, \tag{19}$$

*and its performance is maintained as $\|e\|_2 < \gamma \|d\|_2$ with $\gamma = \max\{\gamma_i\}_{i \in Z_N}$.*

*Proof:* We still assume that the Lyapunov function of the closed-loop system (3) is in the form of (4). If on the switching surface $\mathcal{S}_{ij}$, the inequality (14) holds, which is equivalent to

$$\frac{1}{\mu} X_j(\rho) \leq X_i(\rho) \leq \mu X_j(\rho). \tag{20}$$

Meanwhile, the closed-loop system satisfies the following LMI performance level $\gamma_i$ over each parameter subset $\mathcal{P}_i$

$$\begin{bmatrix} A_{cl,i}^T(\rho,\dot{\rho})X_i(\rho) + X_i(\rho)A_{cl,i}(\rho,\dot{\rho}) + \sum_{k=1}^{s} \{\underline{\nu}_k, \overline{\nu}_k\} \frac{\partial X_i}{\partial \rho_k} + \lambda_0 X_i(\rho) & X_i(\rho)B_{cl,i}(\rho) & C_{cl,i}^T(\rho) \\ B_{cl,i}^T(\rho)X_i(\rho) & -\gamma_i I_{n_d} & D_{cl,i}^T(\rho) \\ C_{cl,i}(\rho) & D_{cl,i}(\rho) & -\gamma_i I_{n_e} \end{bmatrix} < 0, \tag{21}$$

where

$$\begin{bmatrix} A_{cl,i}(\rho,\dot{\rho}) & B_{cl,i}(\rho) \\ C_{cl,i}(\rho) & D_{cl,i}(\rho) \end{bmatrix} = \left[\begin{array}{cc|c} A_i(\rho) & 0 & B_{1,i}(\rho) \\ 0 & 0 & 0 \\ \hline C_{1,i}(\rho) & 0 & D_{11,i}(\rho) \end{array}\right] + \left[\begin{array}{cc} 0 & B_{2,i}(\rho) \\ I & 0 \\ \hline 0 & D_{12,i}(\rho) \end{array}\right] \times \begin{bmatrix} A_{k,i}(\rho,\dot{\rho}) & B_{k,i}(\rho) \\ C_{k,i}(\rho) & D_{k,i}(\rho) \end{bmatrix} \left[\begin{array}{cc|c} 0 & I & 0 \\ C_{2,i}(\rho) & 0 & D_{21,i}(\rho) \end{array}\right].$$

Then the closed-loop system is exponentially stable for every switching signal $\sigma$ with average dwell time (19) and its performance is maintained as $\|e\|_2 < \gamma \|d\|_2$ with $\gamma = \max\{\gamma_i\}_{i \in Z_N}$.

The proof of the exponential stability for average dwell time switching is similar to that in [7] and will be omitted here. In addition, given the initial condition $x_{cl}(0) = 0$, it can be shown from the condition (20)–(21), the inequality

$$\dot{V}_\sigma + \frac{1}{\gamma} e^T e - \gamma d^T d < 0, \qquad \gamma = \max\{\gamma_i\}_{i \in Z_N}$$

holds within each parameter subset. Integrate on both sides of the inequality, we get

$$V_\sigma(x_{cl}(T)) - V_\sigma(x_{cl}(0)) + \frac{1}{\gamma}\|e\|_2^2 - \gamma \|d\|_2^2 < 0.$$

Since $V_\sigma(x_{cl}(T)) \geq 0$ and $V_\sigma(x_{cl}(0)) = 0$, we have $\|e\|_2 < \gamma\|d\|_2$ hold as desired.

Using Elimination lemma, one can verify the equivalence between condition (21) and LMIs (15)–(17). Moreover, when $M_i(\rho) = R_i(\rho)$ and $N_i(\rho) = R_i^{-1}(\rho) - S_i(\rho)$, recall the expression of the Lyapunov function $V_\sigma(x_{cl}, \rho)$ in (9). If switching from the parameter subset $\mathcal{P}_i$ to $\mathcal{P}_j$, it is required that $V_j([x; x], \rho) \leq \mu V_i(x_{cl}, \rho)$ to guarantee the stability condition of switching with average dwell time. Obviously, it is satisfied if $\mu R_j(\rho) \geq R_i(\rho)$. Similarly, $R_i(\rho) \geq \frac{1}{\mu} R_j(\rho)$ is sufficient to hold $V_i([x; x], \rho) \leq \mu V_j(x_{cl}, \rho)$ when switching from the other direction of the switching surface $\mathcal{S}_{ij}$. Combining them together gives the boundary condition (18). *Q.E.D.*

Note that the switching LPV synthesis condition for this switching logic is different from hysteresis switching LPV control results. The $(1, 1)$ term in (15)–(16) implies that the closed-loop switched LPV system has its convergence rate at least $\frac{\lambda_0}{2}$. The open-loop plant can be thought as a shifted system with its $A_i$ matrix changing to $A_i + \frac{\lambda_0}{2} I$. It is the same for controller $A_{k,i}$ matrix. Therefore, if the matrix functions $R_i(\rho)$ and $S_i(\rho)$ can be solved, then the gains of the switching LPV controllers will be constructed by replacing $A_i$ and $A_{k,i}$ in the standard LPV controller formula (10) by $A_i + \frac{\lambda_0}{2} I$ and $A_{k,i} + \frac{\lambda_0}{2} I$.

# 3 Flight Control Example

The system to be controlled is the longitudinal F-16 aircraft model based on NASA Langley Research Center (LaRC) wind tunnel tests [24], which is described by Stevens and Lewis in great detail [25]. In this research, a simple thrust vectoring model is added to the aircraft model and will be activated in the high angle of attack region to provide additional longitudinal axis control power.

## 3.1 Longitudinal Model of F-16 Aircraft with Thrust Vectoring

The states used to describe the motion of the aircraft in longitudinal axis over entire operating envelope are as follows: $V$ (ft/s) is the total aircraft velocity, $\alpha$ (deg) is the angle of attack, $q$ (deg/s) is the pitch rate, and $\theta$ (deg) is the pitch angle. For the original aircraft model, the available control inputs are the throttle setting $\delta_{th}$ and the elevator angle $\delta_e$ (deg). The resulting

nonlinear equations of motion in longitudinal axis are given as follows:

$$\dot{V} = \frac{1}{m}\left(F_x \cos\alpha + F_z \sin\alpha\right) \tag{22}$$

$$\dot{\alpha} = \frac{1}{mV}\left(-F_x \sin\alpha + F_z \cos\alpha\right) + q \tag{23}$$

$$\dot{q} = \frac{M_y}{I_y} \tag{24}$$

$$\dot{\theta} = q, \tag{25}$$

where $m$ is the aircraft mass, $F_x$ and $F_z$ are the force components along $x$ and $z$ body axes respectively, $I_y$ is the moment of inertia about the $y$ body axis, and $M_y$ is the pitching moment. Note that the throttle setting indirectly affects the states through the power output from the engine. Therefore, the actual power level is also considered as a state variable in longitudinal dynamics, and the detailed dynamical model of the engine can be referred in the NASA data. In addition, $V$, $\alpha$, and $q$ are selected as outputs.

The $x$ and $z$ axes forces and pitching moment in Eqs. (22)-(25) contain aerodynamic, gravitational and thrust components.

$$\begin{aligned} F_x &= \overline{q} S C_{x,t} - mg\sin\theta + T_x \\ F_z &= \overline{q} S C_{z,t} + mg\cos\theta + T_z \\ M_y &= \overline{q} S \overline{c} C_{m,t} + M_T, \end{aligned}$$

where $\overline{q}$ is the dynamic pressure, $S$ is the wing surface area, and $\overline{c}$ is the wing mean aerodynamic chord. A complete description of the total coefficients $C_{x,t}$, $C_{z,t}$, and $C_{m,t}$ can be founded in Ref. [24], which also provides the aerodynamic data in tabular form.


(a) Original aircraft model

(b) Aircraft model augmented with thrust vectoring

Figure 3: Aircraft model with and without thrust vectoring.

The F-16 aircraft is powered by an after-burning turbofan jet engine, which produces a thrust force in the $x$ axis direction, as shown in Figure 3(a). In this research, the F-16 aircraft is augmented

with a simple thrust vectoring model, which is similar to that in Ref. [2]. Denote the thrust vector angle by $\delta_{ptv}$, as shown in Figure 3(b). With the right-handed (forward, starboard, and down) coordinate system, the thrust components along the $x$, $z$ axes and the pitching moment due to thrust vector are then given by

$$\begin{aligned} T_x &= T\cos\delta_{ptv} \\ T_z &= -T\sin\delta_{ptv} \\ M_T &= -l_T T\sin\delta_{ptv}, \end{aligned}$$

where $l_T$ is the moment arm from the center of gravity to the thrust application point. A more complicated model of thrust vectoring can be found in Refs. [26, 27], but will not be used in our study.

To develop an LPV representation of the nonlinear F-16 model, we first need to find the wings-level equilibrium points at several flight conditions in the design envelope. The local linear models are then obtained by linearizing the nonlinear equations of motion at those points. The flight envelope of interest covers aircraft speeds between 160 ft/s and 200 ft/s and angles of attack from $20^\circ$ to $45^\circ$. These two variables are used as scheduling parameters in the LPV modeling of F-16 longitudinal dynamics. The points at which the nonlinear model is linearized are marked by a "$\times$" symbol in Figure 4. To apply the switching LPV control synthesis technique, the flight envelope is partitioned into two subregions. For hysteresis-based switching, the striped area in Figure 4(a) is the overlapped parameter region. So there are two switching surfaces, $\alpha = 30^\circ$ and $\alpha = 35^\circ$. For the switching with average dwell time, the overlapped region shrinks to a line. Here, we take the line $\alpha = 33^\circ$ shown in Figure 4(b) as the switching surface.

In this research, two different sets of actuators are used in the different angle of attack regions. The actuators used in the low angle of attack region (region 1), are the throttle and the elevator, and the thrust vectoring nozzle is inactive. The local linear models in this region are based on the original aircraft model, which is corresponding to the case of $\delta_{ptv} = 0$. In the high angle of attack region (region 2), the thrust vectoring nozzle is incorporated to provide additional force and moment. Therefore, the switching of controllers is based on the trajectory of the angle of attack, i.e., the controller is switched only when the aircraft flies from one angle of attack region to the other.

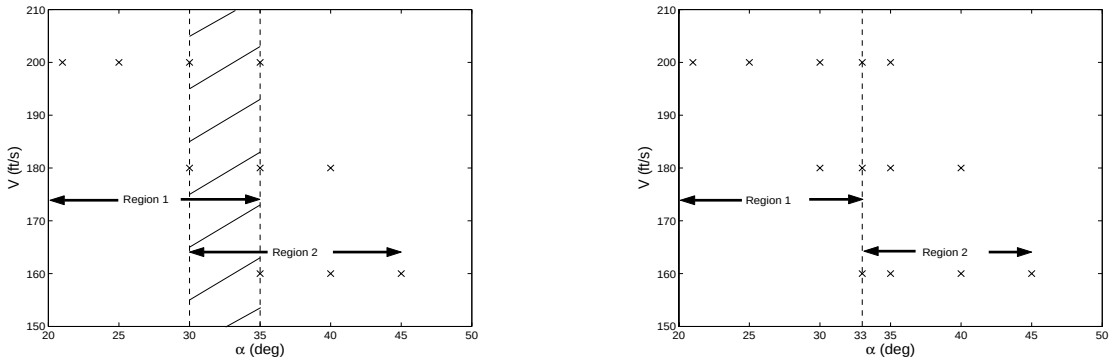


(a) Hysteresis switching

(b) Switching with average dwell time

Figure 4: Flight conditions and partitioned flight envelope for two switching logics.

### 3.2 Control Problem Setup

The control design objective is to track the command of the angle of attack. It is formulated as a model-following problem, where the ideal model to be followed is chosen to be a second-order low-pass filter based on desired flying qualities. A block diagram of the system interconnection for synthesizing the switched LPV controllers is shown in Figure 5, where $P$ is the model set of linearized aircraft dynamics at different trim points, and it has three outputs: the velocity $V$, the angle of attack $\alpha$, and the pitch rate $q$. The inputs of the open-loop system include 3-dimensional sensor noise signal $n$, the angle of attack command $\alpha_{\text{cmd}}$, and the control input $u$. The outputs of the open-loop system are weighted error signals $e_p$ and $e_u$, and the measurement $y$.

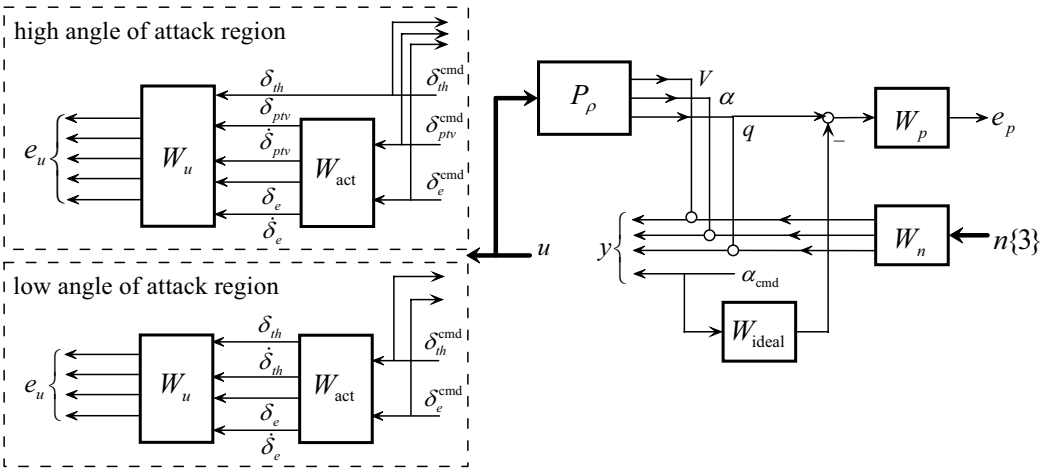


Figure 5: Weighted open-loop interconnection for the F-16 aircraft.

As mentioned before, pilots desire fast and accurate responses in the low angle of attack region.

While in the high angle of attack region, the requirement for the flying quality is not so critical, and the emphasis of the control design is the maintainability of the stability. Therefore, we choose the different performance weighting functions in the different angle of attack regions to reflect design requirements.

$$W_{p1} = \frac{100(s/20+1)}{s/0.1+1}, \qquad W_{p2} = \frac{80(s/10+1)}{s/0.01+1},$$

where the subscripts 1 and 2 denotes the low and high angle of attack region, respectively. Note that the tracking error in the steady state is 1% in the region 1 and 1.25% in the region 2. Also, the bandwidth in the region 1 is greater than that in region 2, and this is consistent with the design objective.

Also, different actuator sets are used in different angle of attack regions. The dynamics of the actuators are modeled as first order lag filters, and the time constants can be found in [24, 2].

$$\frac{\delta_{th}}{\delta_{th}^{\text{cmd}}} = \frac{1}{0.2s+1}, \qquad \frac{\delta_{ptv}}{\delta_{ptv}^{\text{cmd}}} = \frac{1}{0.07s+1}, \qquad \frac{\delta_e}{\delta_e^{\text{cmd}}} = \frac{1}{0.05s+1}.$$

In the low angle of attack region, the control inputs are throttle position $\delta_{th}$ and elevator angle $\delta_e$. Both the positions and the rates of control inputs are fed into $W_u$ to penalize the control effort. Therefore, the system matrix of $W_{\text{act}}$ is given by

$$W_{\text{act}} = \text{diag}\left\{ \left[\begin{array}{c|c} -5 & 5 \\ \hline 1 & 0 \\ -5 & 5 \end{array}\right], \left[\begin{array}{c|c} -20 & 20 \\ \hline 1 & 0 \\ -20 & 20 \end{array}\right] \right\},$$

and the weighting function $W_u$ is given as

$$W_u = \text{diag}\left\{1, 10, \frac{1}{50}, \frac{1}{120}\right\}.$$

In the high angle of attack region, the thrust vector is also activated. In order to use the proposed switching condition, the weighted open-loop LPV plants in the different parameter subspaces must have the same number of the states. Otherwise, the synthesis conditions on the switching surfaces will not hold. Therefore, we ignore the dynamics of the throttle, which has the slowest time constant among the three actuators, and keep the order of $W_{\text{act}}$ as same as that in the low angle of attack region. The related weighting functions $W_{\text{act}}$ and $W_u$ are given as follows.

$$W_{\text{act}} = \text{diag}\left\{ \left[\begin{array}{c|c} -14.28 & 14.28 \\ \hline 1 & 0 \\ -14.28 & 14.28 \end{array}\right], \left[\begin{array}{c|c} -20 & 20 \\ \hline 1 & 0 \\ -20 & 20 \end{array}\right] \right\}, \qquad W_u = \text{diag}\left\{1, \frac{1}{35}, \frac{1}{120}, \frac{1}{50}, \frac{1}{120}\right\}.$$

The other common weighting functions are chosen as

$$W_n = \text{diag}\left\{0.8, 0.1, 0.6\right\}, \qquad W_{\text{ideal}} = \frac{6.25}{s^2 + 3.6s + 6.25},$$

where the ideal model is a second-order system with the natural frequency 2.5 rad/s, and the damping ratio 0.72.

### 3.3 Design Results and Nonlinear Simulations

Two switched LPV controllers corresponding to hysteresis-based and average dwell time switching logics are designed using the proposed switching LPV synthesis conditions in Theorem 1 and 2. The multiple parameter-dependent Lyapunov functions at each parameter subset are parameterized as affine functions of scheduling parameters. That is, we have for $i = 1, 2$

$$R_i(\rho) = R_i^0 + \rho_1 R_i^1 + \rho_2 R_i^2, \qquad S_i(\rho) = S_i^0 + \rho_1 S_i^1 + \rho_2 S_i^2,$$

where $\rho_1 = \alpha$, $\rho_2 = V$, and matrices $R_i^k$ and $S_i^k$ with $k = 0, 1, 2$ are new optimization variables to be determined. The general objective function to optimize is defined as $\min \sum_{i=1}^{Z_N} w_i \gamma_i$, where $w_i$ is the weight to penalize $\gamma_i$ and $\sum_{i=1}^{Z_N} w_i = 1$. In this paper, we define the objective function as $\min \max\{\gamma_1, \gamma_2\}$, which means minimizing the "worst-case" performance level $\gamma_i$. The performance level $\gamma$ over the whole parameter set are 7.9913 for hysteresis switching logic, and 15.9914 for average dwell time switching with $\lambda_0 = 0.01$ and $\mu = 1.1$.

For the switching with average dwell time, the influence of the constants $\lambda_0$ and $\mu$ is also studied by comparing five different sets of values listed in Table 1. The data in the first row are those used in the previous control design and the next nonlinear simulation. We first keep $\lambda_0$ fixed at 0.01, and change the value of $\mu$. It is noticed that the variation of $\mu$ just changes the value of the average dwell time $\tau_a$, and has no impact on the performance level $\gamma$. This can be explained by the fact that $\mu$ is not involved in the synthesis conditions (15)–(18), and thus not related to the value of $\gamma$. We then keep $\mu = 1.1$ and let $\lambda_0$ vary. The performance level $\gamma$ is improved if $\lambda_0$ decreases, but the resulted optimization problem for the case of $\lambda_0 = 0.05$ is infeasible. It is still an open question to determine suitable values of $\lambda_0$ and $\mu$. One possible way is to try and obtain an acceptable performance level as well as a reasonable average dwell time value.

To test the performance of the switching control system during the nonlinear simulation, two angle of attack command inputs are defined as shown in Figure 6. The initial angle of attack command is

Table 1: Effect of constants $\lambda_0$ and $\mu$ on average dwell time switching.

| $\lambda_0$ | $\mu$ | $\tau_a$ | $\gamma$ |
|---|---|---|---|
| 0.01 | 1.1 | 9.53 | 15.9914 |
| 0.01 | 1.05 | 4.88 | 15.9914 |
| 0.01 | 1.5 | 40.55 | 15.9914 |
| 0.001 | 1.1 | 95.31 | 8.4199 |
| 0.05 | 1.1 | 1.91 | infeasible |

selected as 36°, and thus the initial switching signal $\sigma(0) = 2$. The trajectory of the angle of attack command is defined as square waves, and deliberately chosen to cross the two parameter subsets back and forth to illustrate the effect of switching LPV control. There are four switching events happened. For the first command, the switches occur at 0 s, 15 s, 31 s, and 45 s, respectively. Therefore, all the time intervals between switches satisfy the requirement $\tau_a > 9.53$ s. To see the effect of the average dwell time $\tau_a$, we defined another command input which switches fast at the beginning and then compensates by switching sufficiently slow. The switches occur at 0 s, 5 s, 10 s, and 45 s, respectively, and thus the average dwell time still satisfy the requirement. Note that the switching time of the actual angle of attack trajectory is slightly different from the command input, since we try to track the response of a second-order ideal model, not the square wave.

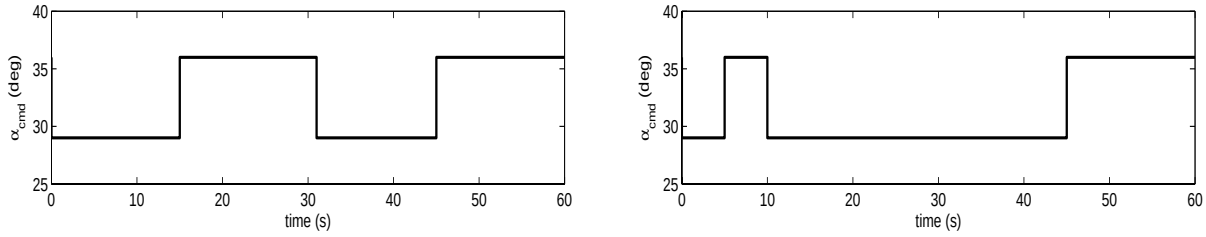


(a) Command input 1

(b) Command input 2

Figure 6: Command inputs for switching LPV control simulation.

The test flight condition is selected at $V = 180$ ft/s and $\alpha = 36°$. Figure 7 shows the nonlinear responses of the aircraft model for the command input 1. The dotted lines in subplot (a) represent the angle of attack response of the ideal model, the solid and dashed lines in all subplots represent the responses using hysteresis switching and average dwell time switching, respectively. The tracking performances over the entire time history are acceptable for both switching logics.

It is noticed that the switching signal $\sigma$ in subplot (b) is a little different for those two switching logics, since their switching surfaces are different. For hysteresis switching, the switch event occurs when $\alpha = 30^\circ$ or $35^\circ$. While for average dwell time switching, there is only one switching surface $\alpha = 33^\circ$. The responses of the actuators are shown in subplots (d)–(f). Obviously, the thrust vector is activated only when the aircraft flies in the high angle of attack region.

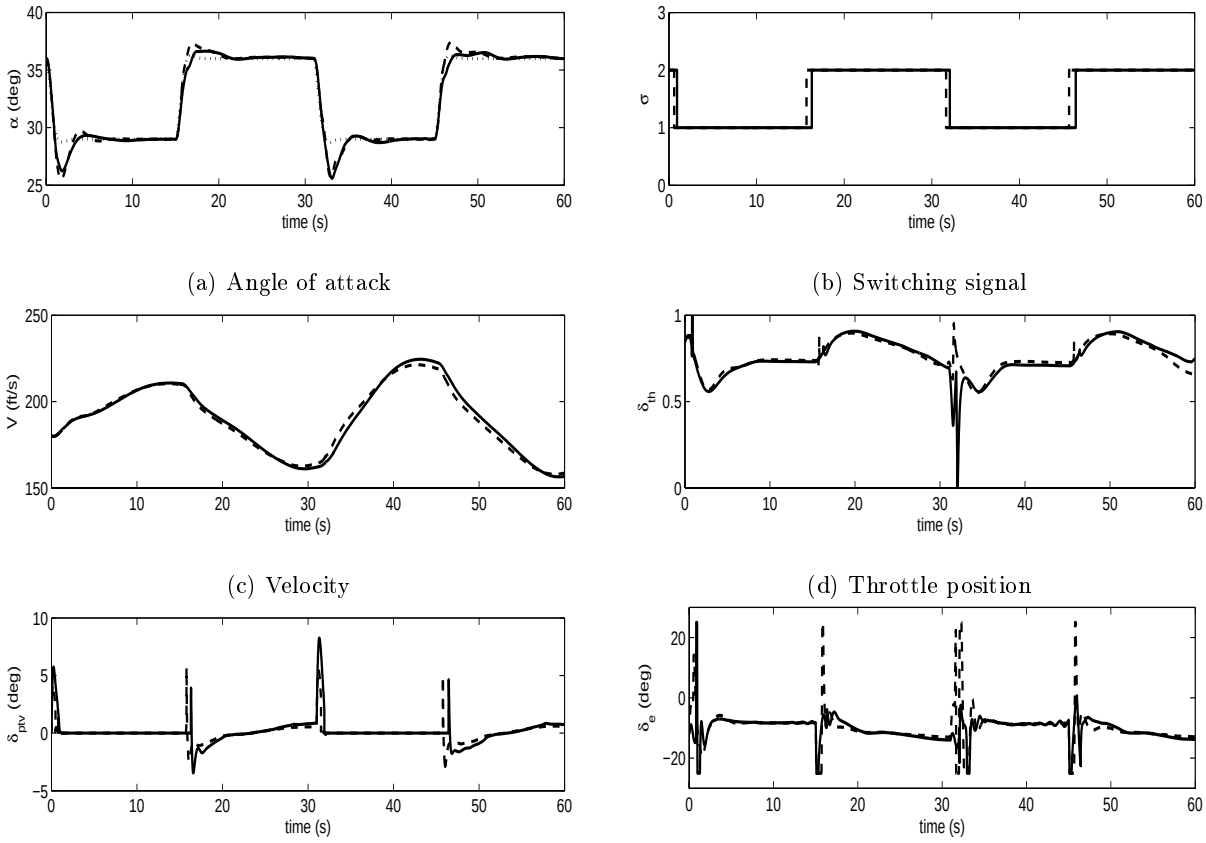


(a) Angle of attack

(b) Switching signal

(c) Velocity

(d) Throttle position

(e) Thrust vectoring nozzle deflection

(f) Elevator angle

Figure 7: Nonlinear simulation of switching LPV control for command input 1.

Figure 8 presents the nonlinear response to the command input 2. For the second switching logic, although the first two switch events occur too fast, the average dwell time still satisfies the requirement (19). Therefore, the tracking performance of switching with average dwell time is also acceptable and a little bit worse than that achieved by the hysteresis switching. However, the stability of the switched system will not be guaranteed if the condition of the average dwell time is violated. Compared to the average dwell time switching, there is no such a restriction on the hysteresis switching. In addition, according to the theoretical developments and the simulation results, the switching with average dwell time appears more complicated than the hysteresis switching

since one has to choose the parameter $\lambda_0$ and $\mu$. Thus the hysteresis switching scheme seems more flexible and has a potential for the high performance aircraft applications.

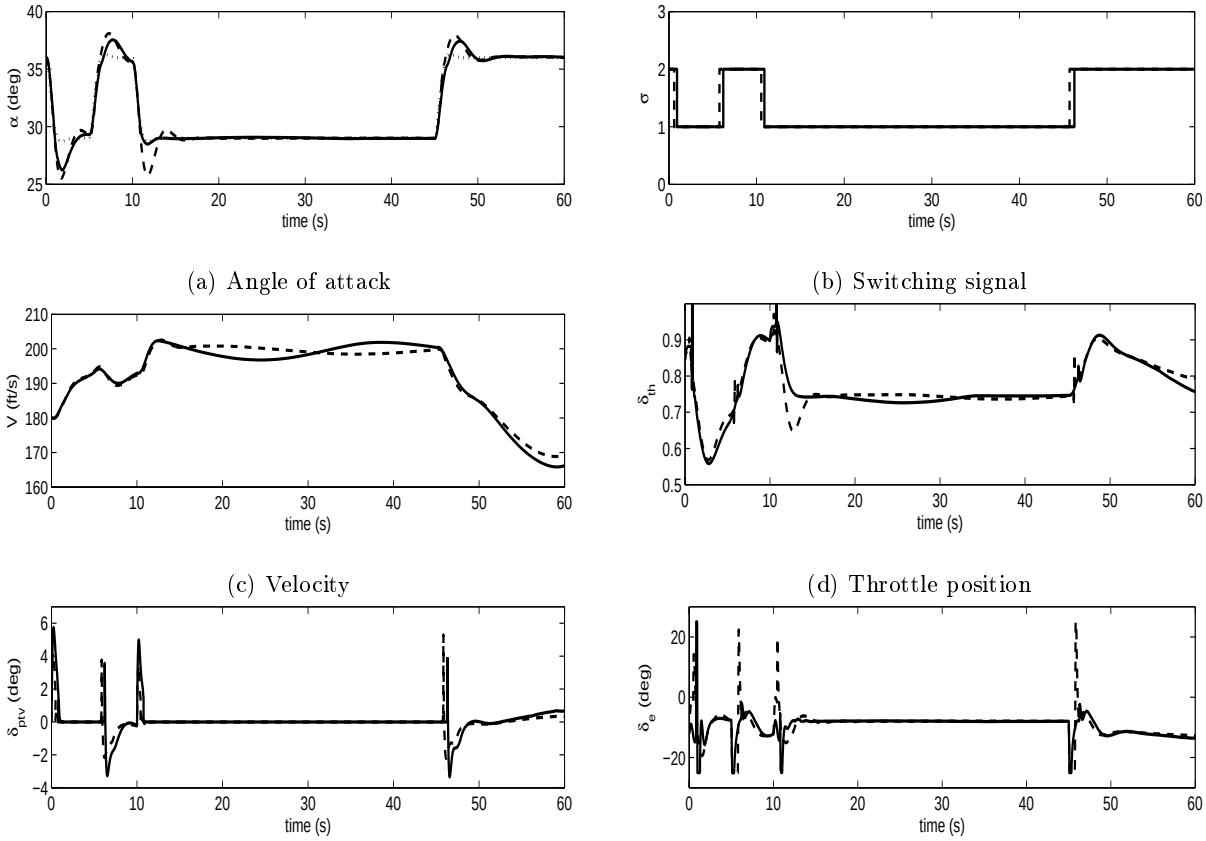


(a) Angle of attack

(b) Switching signal

(c) Velocity

(d) Throttle position

(e) Thrust vectoring nozzle deflection

(f) Elevator angle

Figure 8: Nonlinear simulation of switching LPV control for command input 2.

# 4 Conclusion

A switching LPV control approach based on multiple parameter-dependent Lyapunov functions is presented for flight control design. The state of the controller is reset to the value of the plant state when the switching event occurs. The controller state reset not only guarantees the stability requirement of Lyapunov function, but also leads to the formulation of switching LPV control synthesis conditions as LMI optimization problems. Two parameter-dependent switching logics, hysteresis-based switching and switching with average dwell time, are used to avoid the possible transient instability caused by switching among controllers. The proposed switching LPV control technique is applied to an F-16 aircraft model switching between low and high angle of attack

regions with different control objectives and actuator sets, and promising simulation results are obtained.

## References


[1] J.M. Buffington, A.G. Sparks, and S.S. Banda, "Robust longitudinal axis flight control for an aircraft with thrust vectoring," *Automatica*, Vol. 30, No. 10, pp. 1527–1540, 1994.

[2] J.M. Buffington and D.F. Enns, "Flight control for mixed-amplitude commands," *International Journal of Control*, Vol. 68, No. 6, pp. 1209–1229, 1997.

[3] W.C. Reigelsperger, K.D. Hammett, and S.S. Banda, "Robust control law design for lateral-directional modes of an F-16/MATV using $\mu$-synthesis and dynamic inversion," *International Journal of Robust and Nonlinear Control*, Vol. 7, No. 8, pp. 777–795, 1997.

[4] W.C. Reigelsperger and S.S. Banda, "Nonlinear simulation for a modified F-16 with full-envelope control laws," *Control Engineering Practice*, Vol. 6, No. 3, pp. 309–320, 1998.

[5] R.A. DeCarlo, M.S. Branicky, S. Pettersson, and B. Lennartson, "Perspectives and results on the stability and stabilizability of hybrid systems," *Proceedings of the IEEE*, Vol. 88, No. 7, pp. 1069 - 1082, 2000.

[6] D. Liberzon and A. Morse, "Basic problems in stability and design of switched systems," *IEEE Control Systems Magazine*, Vol. 19, No. 5, pp. 59–70, 1999.

[7] D. Liberzon, *Switching in Systems and Control*, Birkhäuser, Boston, MA, 2003.

[8] S.P. Boyd and Q. Yang, "Structured and simultaneous Lyapunov functions for system stability problems," *International Journal of Control*, Vol. 50, No. 6, pp. 2215–2240, 1989.

[9] M. Johansson and A. Ranzer, "Computation of piecewise quadratic Lyapunov functions," *IEEE Transactions on Automatatic Control*, Vol. 43, No. 4, pp. 555–559, 1998.

[10] P. Peleties and R. Decarlo, "Asymptotic stability of m-switched systems using Lyapunov-like functions," in *Proc. 1991 American Control Conference*, 1991, pp. 1679–1684.

[11] S. Prajna and A. Papachristodoulou, "Analysis of switched and hybrid systems–Beyond piecewise quadratic methods," in *Proc. 2003 American Control Conference*, Denver, CO, June 2003, pp. 2779–2784.

[12] M.A. Wicks, P. Peleties, and R.A. DeCarlo, "Construction of piecewise Lyapunov functions for stabilizing switched systems," in *Proc. 33rd IEEE Conference on Decision and Control*, Dec. 1994, pp. 3492–3497.

[13] M. Branicky, "Multiple Lyapunov functions and other analysis tools for switched and hybrid systems," *IEEE Transactions on Automatic Control*, Vol. 43, No. 4, pp. 475–482, 1998.

[14] H. Ye, A.N. Michel, and L. Hou, "Stability theory for hybrid dynamical systems," *IEEE Transactions on Automatic Control*, Vol. 43, No. 4, pp. 461–474, 1998.

[15] S. Lim, *Analysis and Control of Linear Parameter-Varying Systems*, Ph.D. Dissertation, Stanford University, CA, 1999.

[16] S. Lim and K. Chan, "Stability analysis of hybrid linear parameter-varying systems," in *Proc. 2003 American Control Conference*, Denver, CO, June 2003, pp. 4822–4827.

[17] J.P. Hespanha and A.S. Morse, "Stability of switched systems with average dwell-time," in *Proc. 38th IEEE Conference on Decision and Control*, Dec. 1999, pp. 2655–2660.

[18] B. Lu and F. Wu, "Switching LPV control designs using multiple parameter-dependent Lyapunov functions," *Automatica*, Vol. 40, No. 11, pp. 1973–1980, 2004.

[19] K. Zhou, J.C. Doyle, and K. Glover, *Robust and Optimal Control*, Prentice-Hall, Englewood Cliffs, NJ, 1996.

[20] G. Becker and A. Packard, "Robust performance of linear parametrically varying systems using parametrically-dependent linear feedback," *Systems and Control Letters*, Vol. 23, pp. 205–215, 1994.

[21] F. Wu, X.H. Yang, A. Packard, and G. Becker, "Induced $\mathcal{L}_2$ norm control for LPV systems with bounded parameter variation rates," *International Journal of Robust and Nonlinear Control*, Vol. 6, No. 9/10, pp. 983–998, 1996.

[22] P. Gahinet, A. Nemirovskii, A.J. Laub, and M. Chilali, *LMI Control Toolbox*, Mathworks, Natick, MA, 1995.

[23] G. Becker, "Additional results on parameter-dependent controllers for LPV systems," in *Proc. 13th IFAC World Congress*, 1996, pp. 351–356.

[24] L.T. Nguyen, M.E. Ogburn, W.P. Gillert, K.S. Kibler, P.W. Brown, and P.L. Deal, *Simulator Study of Stall/Post-Stall Characteristics of A Fighter Airplane with Relaxed Longitudinal Static Stability*, *NASA Technical Paper* 1538, 1979. http://library-dspace.larc.nasa.gov/dspace/jsp/handle/2002/11034.

[25] B.L. Stevens and F.L. Lewis, *Aircraft Control and Simulation*, John Wiley & Sons, Inc., 1992.

[26] B. Gal-Or and D.D. Baumann, "Mathematical phenomenology for thrust-vectoring-induced agility comparisons," *Journal of Aircraft*, Vol. 30, No. 2, pp. 248-254, 1993.

[27] K.A. Wise and D.J. Broy, "Agile missile dynamics and control," *Journal of Guidance, Control, and Dynamics*, Vol. 21, No. 3, pp. 441-449, 1998.